

## SUBSTRATE EFFECT ON THE STRUCTURAL AND ELECTROCHEMICAL PROPERTIES OF ELECTROLYTIC MANGANESE DIOXIDE DEPOSITED FROM SULPHATE SOLUTIONS

Avijit Biswal<sup>1,2</sup>, Abhijeet Singh<sup>3</sup>, \*B.C Tripathy<sup>1,2</sup>, K. Sanjay<sup>1</sup>, T. Subbaiah<sup>1,2</sup>, B.K. Mishra<sup>1</sup>

<sup>1</sup>*CSIR - Institute of Minerals and Materials Technology,  
Council of Scientific and Industrial Research, Bhubaneswar-751013, India  
(\*Corresponding author: [bankimtripathy@gmail.com](mailto:bankimtripathy@gmail.com))*

<sup>2</sup>*Academy of Scientific and Innovative Research,  
Anusandhan Bhavan, Rafi Marg, New Delhi-110 001, India*

<sup>3</sup>*National Institute of Technology-Durgapur, West Bengal, India*

### ABSTRACT

We studied the effect of anode substrates such as pure lead (Pb), lead antimony (Pb-Sb), and lead-silver (Pb-Ag) on the structural and electrochemical properties of electrolytic manganese dioxide (EMD). X-ray diffraction (XRD), field emission scanning electron microscopy (FESEM), and chemical analyses were used to determine the structural and chemical characteristics of the EMD samples. The charge–discharge profile was studied in 9 M KOH using a galvanostatic charge-discharge unit. In all the substrates the current efficiencies were more than 99% except with Pb-Sb where it was 90%. Results revealed the nature of the substrate strongly affected the morphology of the deposited material which in turn affected the electrochemical properties of the EMD samples. XRD analyses revealed that the nature of the anode did not affect the crystal structure of the deposited EMD and all the samples were predominantly  $\gamma$ -MnO<sub>2</sub>, which is electrochemically active for energy storage applications. The EMD deposited on lead substrate showed superior discharge capacity of 245 mAhg<sup>-1</sup> when compared with other substrates.

### KEYWORDS

Electrolytic manganese dioxide, anode substrate, morphology, discharges capacity.

## INTRODUCTION

Use of manganese dioxide/Zn ( $\text{MnO}_2/\text{Zn}$ ) batteries in a Laclanche cell is not new but after the improvement of the Laclanche cell for alkaline batteries, this system ( $\text{MnO}_2/\text{Zn}$ ) conquered the market due to its low cost, good self life, high temperature performance and ecofriendly nature (Kordesch, 1960; Kordesch, 1978; Kordesch & Weissenbacher, 1994; Marsal, Kordesch, & Urry, 1960). Despite increasing competition from the rechargeable batteries, the primary Zn/Mn batteries, which were manufactured using electrolytic manganese dioxide (EMD) as essential raw material, were expected to remain dominant in the household markets for its relative convenience and low initial cost till today. EMD is prepared by anodic oxidation of manganese sulfate in sulfuric acid solution. The concentration of  $\text{MnSO}_4$  and  $\text{H}_2\text{SO}_4$  are taken in the ratio of 2:1 (Farris & Martin, 2004). Electrodeposition of manganese dioxide is influenced by various parameters such as concentration of electrolyte, current density, pH of the electrolyte and the temperature of the electrolytic bath, apart from this the anode material also play an important role in modifying the structure and properties of EMD. The selection of suitable anode material for the deposition of EMD has been briefly highlighted by Rethinaraj and Visvanathan (1991). It is reported that pure titanium is found to be very attractive anode for the preparation of electro inorganic chemicals, like EMD. Hence in terms of the economical point of view, an attempt is made to investigate the effect of lead based anode substrate on the structure and properties of EMD deposited from synthetic manganese sulphate solution.

## EXPERIMENTAL

### Materials and Methods for Producing EMD

Electrolytic manganese dioxide (EMD) was prepared from synthetic aqueous sulfate solutions containing  $50 \text{ g dm}^{-3}$   $\text{MnSO}_4 \cdot 7\text{H}_2\text{O}$  and  $25 \text{ g dm}^{-3}$   $\text{H}_2\text{SO}_4$  at an anodic current density of  $200 \text{ A m}^{-2}$  in a glass cell. A schematic diagram of the electrolytic cell arrangement is shown in Figure 1. The anodic oxidation of  $\text{Mn}^{2+}$  to  $\text{MnO}_2$  was carried out on various anodes (rolled) like lead (Pb), lead-antimony (Pb-Sb, (Sb-6%), or lead-silver (Pb-Ag)(Ag-1%) placed in parallel to a stainless steel (SS) cathode in their individual experiments. All experiments were carried out at  $90\text{--}92^\circ\text{C}$  for 6 h. EMD samples deposited on various substrates such as Pb, Pb-Sb and Pb-Ag have been labeled as  $\text{EMD}_{\text{Pb}}$ ,  $\text{EMD}_{\text{Pb-Sb}}$  and  $\text{EMD}_{\text{Pb-Ag}}$ , respectively. The electrodeposited  $\text{MnO}_2$  was removed from the anode after the deposition period and washed thoroughly with deionized water before drying in an oven. The dried mass was ground and sieved through a  $100\text{-}\mu\text{m}$  mesh to obtain EMD powder. Subsequently, the resultant product in powder form was washed repeatedly with deionized water until the sample was sulfate free. The EMD powder was finally dried and cooled in a desiccator and subjected to physical and electrochemical characterization. Morphological characterization was performed on the EMD flakes, those scrapped off the anodes. These were washed with deionized water before analysis.

### Structural Characterization

X-ray diffractograms were recorded for the EMD powders using PANalytical diffractometer (PW 1830; Philips, Japan) with  $\text{Mo K}\alpha$  radiation,  $\lambda = 0.71073 \text{ \AA}$ . The scans were recorded in  $2\theta$  range  $5\text{--}45^\circ$ . Field emission scanning electron microscope (FESEM) (ZEISS SUPRA 55) was used to examine the surface morphology of the EMD samples.

### Electrochemical Characterization

Electrochemical characterization was carried out in a floated cell arrangement. The experimental cell consisted of a zinc strip as anode, and the cathode was in the form of a pellet, made from a uniform mixture of EMD and graphite powder (4:1), with 2–3 drops of 5 % polyvinyl alcohol as binder. The mixture was placed in a stainless steel mesh meant for electrical contact and then subjected to a pressure of 12 t for 3 min by means of a pelletiser (KBr press) in a 20 mm die. The pellet was put into a cell assembly in an electrolyte of 9M potassium hydroxide (KOH) and allowed to equilibrate for 1 h at its open circuit

potential. Discharging was done at a current of 20 mA with a cutoff voltage of 0.9 using a deep cycle battery tester (Bitrode, USA).

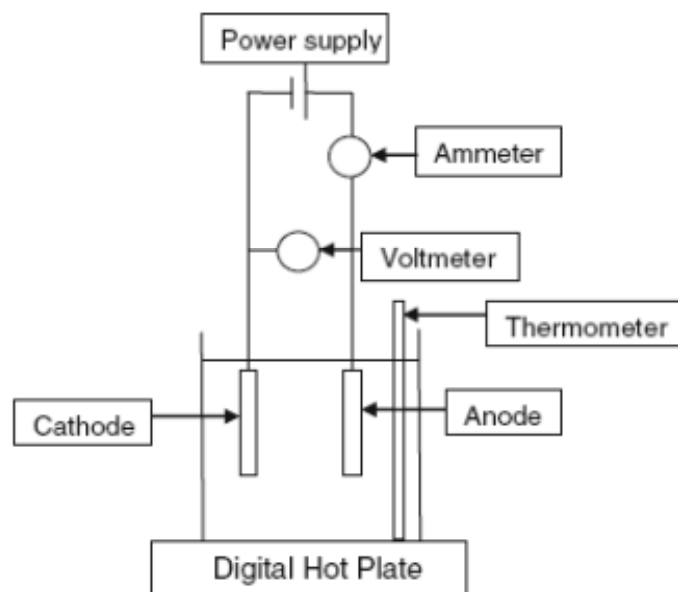
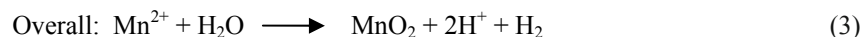
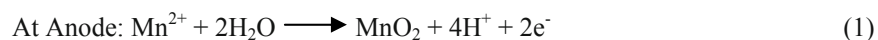


Figure 1-Schematic diagram of electrolytic cell arrangement for depositing EMD

## RESULTS AND DISCUSSIONS

### Electrodeposition of Manganese Dioxide

Electrooxidation of  $\text{MnO}_2$  was performed at an anodic current density of  $0.02 \text{ A cm}^{-2}$  for 6 h from the electrolyte containing about  $50 \text{ g dm}^{-3}$  manganese with  $25 \text{ g dm}^{-3}$  of  $\text{H}_2\text{SO}_4$ . The electrodeposition of manganese dioxide from  $\text{MnSO}_4\text{-H}_2\text{SO}_4$  solution can be represented by the following steps:



As shown in Figure 2 for both  $\text{EMD}_{\text{Pb}}$  and  $\text{EMD}_{\text{Pb-Ag}}$  the current efficiencies (C.E.) are 99% whereas  $\text{EMD}_{\text{Pb-Sb}}$  is 90%. Likewise, Figure 3 shows that the energy consumption (E.C.) is a minimum for  $\text{EMD}_{\text{Pb}}$  (1.337 kWh/kg) in comparison to that of  $\text{EMD}_{\text{Pb-Sb}}$  (1.788 kWh/kg) and  $\text{EMD}_{\text{Pb-Ag}}$  (1.48 kWh/kg).

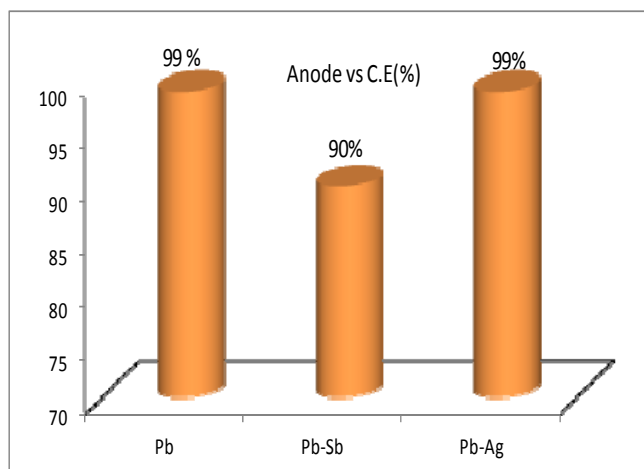


Figure 2 - Effect of anode substrate on C.E during electrodeposition of manganese dioxide

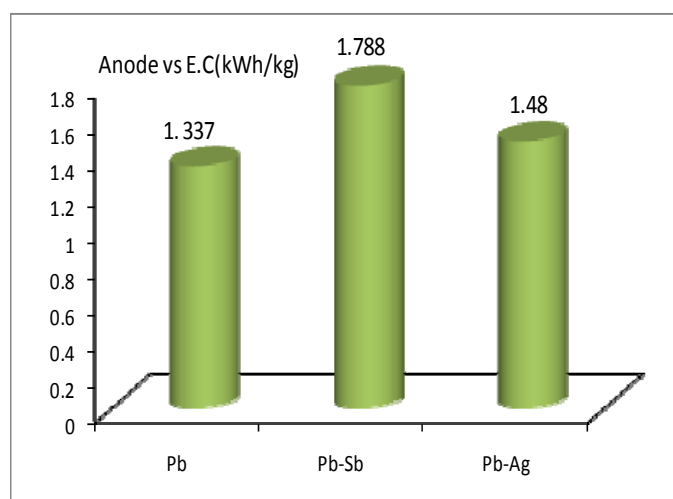


Figure 3 - Effect of anode substrate on E.C. during electrodeposition of manganese dioxide

### X-ray Diffraction Analysis

X-ray diffractograms of the EMD samples deposited on the three lead anode substrates are shown in Figure 4. All the observed diffraction peaks can be indexed to an orthorhombic phase of  $\gamma$ - $\text{MnO}_2$  with lattice constants  $a = 8.70 \text{ \AA}$ ,  $b = 2.90 \text{ \AA}$ , and  $c = 4.41 \text{ \AA}$ . These are in good agreement with the standard values (JCPDS card no. 65-1298;  $a = 9.27 \text{ \AA}$ ,  $b = 2.87 \text{ \AA}$ ,  $c = 4.53 \text{ \AA}$ ). The peaks at  $2\theta$  values of approximately  $10^\circ$ ,  $16^\circ$ ,  $19^\circ$ ,  $24^\circ$  and  $29^\circ$  correspond to the (120), (131), (300), (160), and (421) planes of  $\gamma$ - $\text{MnO}_2$ , respectively. All three EMD samples ( $\text{EMD}_{\text{Pb}}$ ,  $\text{EMD}_{\text{Pb-Sb}}$ , and  $\text{EMD}_{\text{Pb-Ag}}$ ) were found to contain  $\gamma$ -phases, with good crystalline behavior. No significant difference is observed among the three types of EMD samples, hence it can be concluded that if electrolytic deposition conditions are constant, the crystal pattern of deposited EMD will be the same regardless the variable anode substrate.

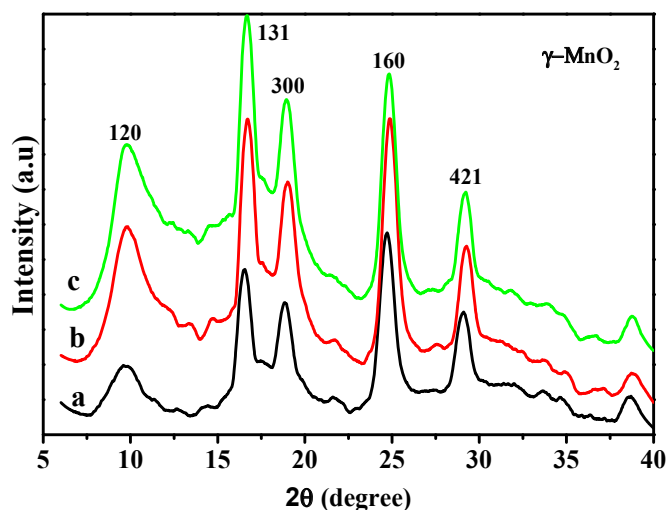


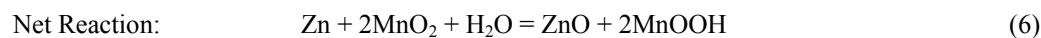
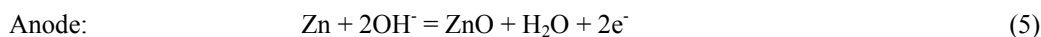
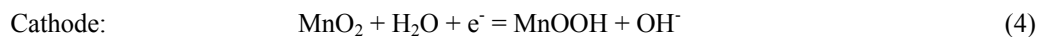
Figure 4 - X-ray diffraction pattern of EMD material deposited on (a) Pb anode (b)Pb-Sb anode and (c) Pb-Ag anode.

### Surface Morphology of the EMD

The three types of EMD samples ( $\text{EMD}_{\text{Pb}}$ ,  $\text{EMD}_{\text{Pb-Sb}}$ , and  $\text{EMD}_{\text{Pb-Ag}}$ ) were investigated by FESEM. It is interesting to note that in all cases, the particle size was in the nano range (~50 to 100 nm), and the particles formed a net-like arrangement during electrodeposition. Although no differences were seen in the XRD for the EMD samples, their morphology appeared to be significantly different. The individual particles of  $\text{EMD}_{\text{Pb}}$  (Figure 5a) obtained during electrodeposition consisted of star-shaped particles with four appendages arranged in a netlike fashion. A similar observation of synthesized  $\gamma\text{-MnO}_2$  deposited electrolytically was recorded by Chen, Zhu, Han, Zheng, Yang, & Wang (2009).  $\text{EMD}_{\text{Pb-Sb}}$  (Figure 5b) samples show spindle-shaped particles with consecutive occurrence of some agglomerated round shaped particles. However it is interesting to note that  $\text{EMD}_{\text{Pb-Ag}}$  (Figure 5c) show spindle-shaped particles which are covered by another layer.

### Electrochemical Activity

The suitability of the EMDs as battery materials prepared by varying the anode substrates was assessed by discharge behavior (Figure 6) through imposing a constant current over a period of time.  $\text{MnO}_2$  as a half-cell versus metallic Zn was used. The samples were subjected to discharge studies in 9 M potassium hydroxide aqueous solutions. The reactions at cathode and anode are shown in reactions 4-6.



The first electron of  $\text{MnO}_2$  is allowed to discharge via the homogeneous reversible reaction by the movement of protons and electrons into the lattice, resulting in the reduction of  $\text{MnO}_2$  to  $\text{MnO}_{1.5}$  (Kordes, Gsellmann, Peri, Tomantschger, & Chemelli, 1981; Minakshi, 2008; Minakshi, Singh, Carter, & Prince, 2008). This could be possible due to the conversion of  $\text{MnO}_2$  into  $\text{MnOOH}$  in the solid phase. The second electron discharge of  $\text{MnO}_2$ , proceeds either in solid or in solution phase, leads to the formation of  $\text{Mn}(\text{OH})_2$  containing soluble Mn (II) species, which is formed during recharging of  $\gamma\text{-MnO}_2$  (Mondolini, Laborde, Rioux, Andoni, & Levy-Clement, 1992; Ruetschi, 1984). The formation of the

discharged products is reported to be nonreversible. This system is, therefore, suitable only as a use and dispose battery. Urfer, Lawrence, & Swinkles (1997) reported that the proton–electron pair formed during the discharge process diffuses from the EMD surface to the interior of the material. They maintained that the diffusion rate of the proton–electron pair is a function of the structural, physicochemical, and electrochemical properties of the EMD (Urfer et al., 1997). The theoretical discharge capacity of EMD has been reported as  $308 \text{ mAh g}^{-1}$  with regard to one electron discharge step (Li, Wang, He & Zhou, 2010). The discharge capacities versus cell voltage profile of the EMD samples are shown in Figure 6.  $\text{EMD}_{\text{Pb}}$  and  $\text{EMD}_{\text{Pb-Sb}}$  show discharge capacities of  $\sim 245$  and  $\sim 227 \text{ mAhg}^{-1}$ , respectively, whereas  $\text{EMD}_{\text{Pb-Ag}}$  shows a discharge capacity of  $\sim 215 \text{ mAh g}^{-1}$ .

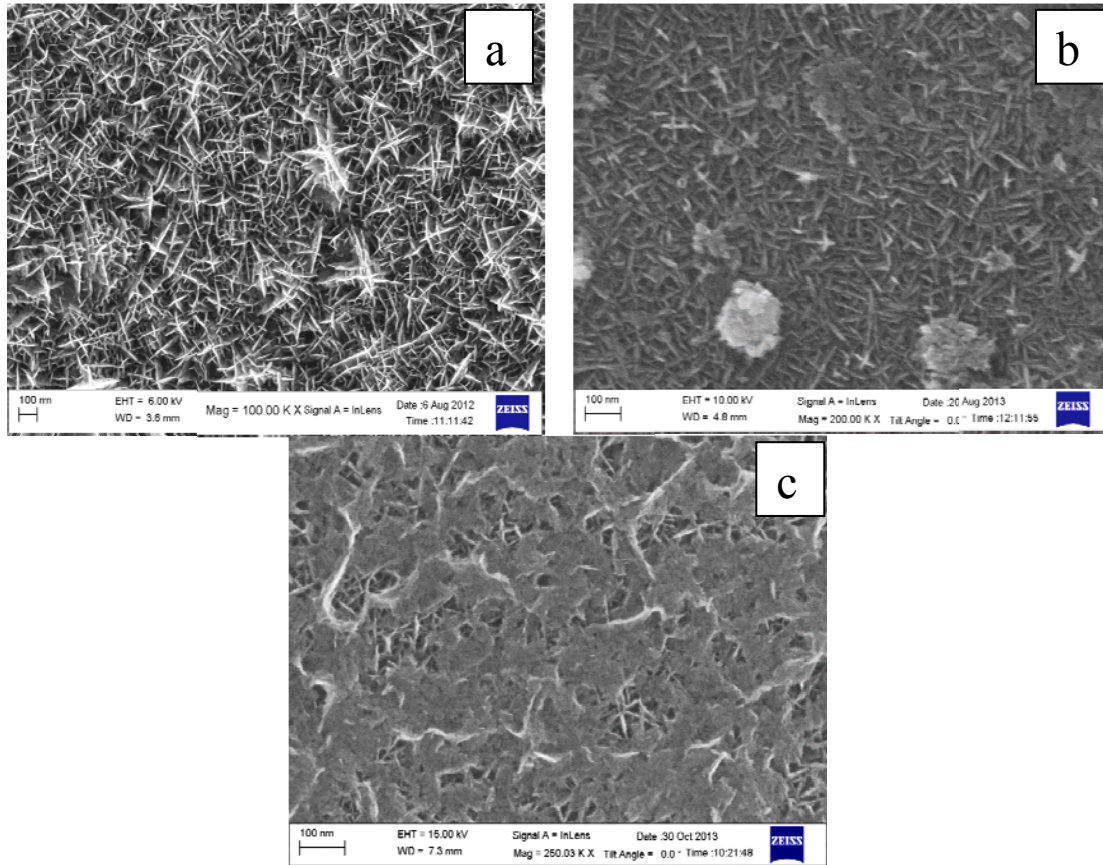


Figure 5 - FESEM images of EMD samples (a) $\text{EMD}_{\text{Pb}}$  (b) $\text{EMD}_{\text{Pb-Sb}}$  (c) $\text{EMD}_{\text{Pb-Ag}}$ .

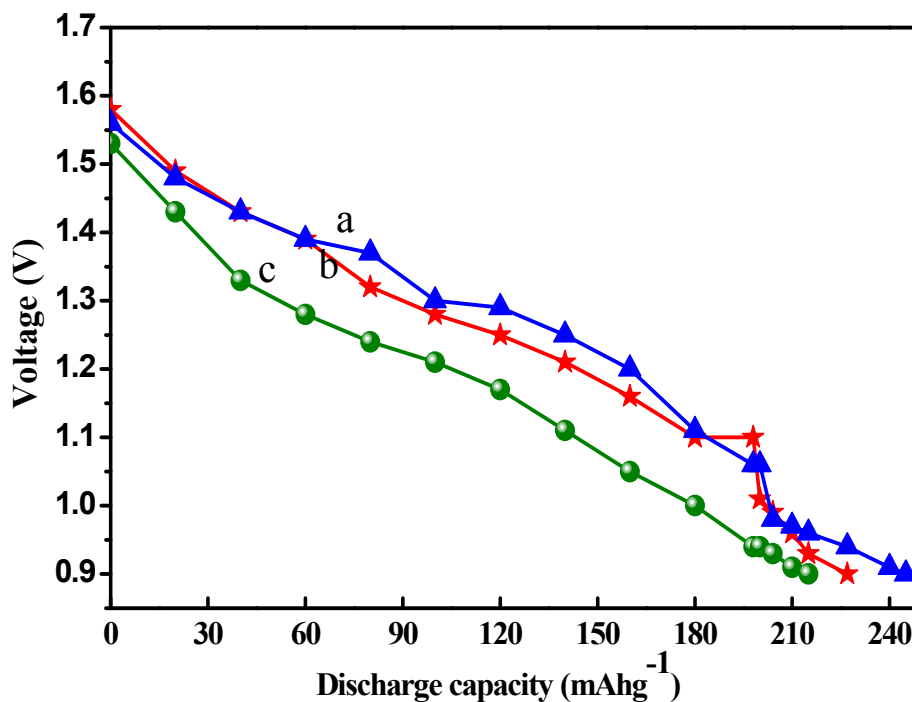


Figure 6 - Plots showing the discharge capacities of the EMD samples obtained from (a) EMD<sub>Pb</sub>, (b) EMD<sub>Pb-Sb</sub> (c) EMD<sub>Pb-Ag</sub>

### CONCLUSIONS

The effect of the anode substrate on the structural and electrochemical behavior of the EMDs produced from synthetic manganese sulphate solutions were reported, and the following conclusions were drawn:

- All the samples show characteristics of  $\gamma$ -MnO<sub>2</sub> which is essential for their electrochemical activity and variation of the anode substrate did not affect the crystal phase of the deposited material.
- FESEM images show that the EMDs deposited on substrates have different surface morphologies, indicating a significant effect of the substrate interface on the shapes and sizes of the EMD particles.
- Tetra-branched star shaped nano particles were obtained for EMD<sub>Pb</sub>, spindle shaped nano particles with frequent appearance of round shaped particles for EMD<sub>Pb-Sb</sub>, and needle like growth of nano particles covered with another layer for EMD<sub>Pb-Ag</sub> were also seen.
- EMD<sub>Pb</sub> shows superior discharge capacity of 245 mAhg<sup>-1</sup> against the discharge capacity of 227 and 215 for EMD<sub>Pb-Sb</sub> and EMD<sub>Pb-Ag</sub> respectively.

### ACKNOWLEDGEMENTS

The authors would like to thank the Director of CSIR-IMMT for his interest and encouragement in publishing this work. One of the authors (A.B.) would like to thank CSIR for providing Senior Research Fellowship for carrying out his doctoral research. This research was partly supported by Ministry of Earth Sciences, Govt. of India.



## REFERENCES

- Chen S, Zhu J, Han Q, Zheng Z, Yang Y, & Wang X (2009). Shape controlled synthesis of one dimension  $\text{MnO}_2$  via a facile quick precipitation procedure and its electrochemical properties. *Crystal Growth and Design*, 9, 4356–4361. doi: 10.1021/cg900223f.
- Farris, J., & Martin, S. (2004). *Electrodeposition of manganese dioxide* (Technical Report). Department of Materials Science and Engineering, Michigan Technological University, 3110 April 28 Technical Report .
- Kordesch, K. (1960). US Patent No. 2,962,540. Washington, DC: U.S. Patent and Trademark Office.
- Kordesch, K. (1978). US Patent No. 4 091 178. Washington, DC: U.S. Patent and Trademark Office.
- Kordesch K, Gsellmann J, Peri M, Tomantschger K, & Chemelli R (1981) . The rechargeability of manganese dioxide in alkaline electrolytes. *Electrochim Acta*, 26, 1495–1504. doi: 10.1016/0013-4686(81)90021-9.
- Kordesch, K., & Weissenbacher, M., (1994). Rechargeable alkaline manganese dioxide/Zinc batteries. *J. Power Sources*, 51, 61-78. doi: 10.1016/0378-7753(94)01955-X.
- Li , H, Wang, Y, He, P, & Zhou, H (2010). A novel rechargeable Li-AgO battery with hybrid electrolytes. *Chem Comm* 46, 2055–2057. doi: 10.1039/B923706B.
- Marsal, P.A., Kordesch, K.V., & Urry, L.F. (1960). US Patent No. 2,960,558. Washington, DC: U.S. Patent and Trademark Office.
- Minakshi M., (2008). Examining manganese dioxide electrode in KOH electrolyte using TEM technique, *J Electroanal Chem.* 616, 99–106. doi:10.1016/j.jelechem.2008.01.011.
- Minakshi M, Singh P, Carter M, & Prince K, (2008). The Zn– $\text{MnO}_2$  sub Battery: The influence of aqueous LiOH and KOH electrolytes on the intercalation mechanism, *Electrochem Solid State Lett* , 11, A145–A149. doi:10.1149/1.2932056.
- Mondolini C, Laborde M, Rioux J, Andoni E, & Levy-Clement C (1992). Rechargeable manganese dioxide batteries: I. In situ X-ray diffraction investigation of the  $\text{H}^+/\gamma\text{MnO}_2$  (EMD type) Insertion system. *J Electrochem Soc* 139, 954–959. doi:10.1149/1.2069374.
- Rethinaraj, J.P., & Visvanathan, S. (1991). Anodes for the preparation of EMD and application of  $\text{MnO}_2$  coated anodes for electrochemicals. *Materials Chemistry. and Physics.*, 27, 337-349. doi: 10.1016/0254-0584(91)90131-D.
- Ruetschi, P. (1984). Cation Vacancy model for  $\text{MnO}_2$ . *J Electrochem Soc* 131, 2737–2744. doi:10.1149/1.2115399.
- Urfer A, Lawrence GA, & Swinkles DAJ (1997). Measuring variation in EMD reduction with location in primary alkaline batteries. *J Appl Electrochem*, 27, 667–672. doi:10.1023/A:1018479502757.